Resonating Valence Bond States in an Electron-Phonon System

Zhaoyu Han and Steven A. Kivelson
Department of Physics, Stanford University, Stanford, California 94305, USA

(Received 2 November 2022; accepted 14 April 2023; published 3 May 2023)

We study a simple electron-phonon model on square and triangular versions of the Lieb lattice using an asymptotically exact strong coupling analysis. At zero temperature and electron density $n = 1$ (one electron per unit cell), for various ranges of parameters in the model, we exploit a mapping to the quantum dimer model to establish the existence of a spin-liquid phase with $\mathbb{Z}_2$ topological order (on the triangular lattice) and a multicritical line corresponding to a quantum critical spin liquid (on the square lattice). In the remaining part of the phase diagram, we find a host of charge-density-wave phases (valence-bond solids), a conventional s-wave superconducting phase, and with the addition of a small Hubbard U to tip the balance, a phonon-induced d-wave superconducting phase. Under a special condition, we find a hidden pseudospin $SU(2)$ symmetry that implies an exact constraint on the superconducting order parameters.

DOI: 10.1103/PhysRevLett.130.186404

The electron-phonon interaction plays an essential role in the physics of quantum materials, e.g., for Bardeen-Cooper-Schrieffer superconductivity (SC) and typical charge or bond-density-wave ordering [1–3]. In the past few years, it has become increasingly clear that electron-phonon interactions can also induce a variety of more exotic behaviors and novel quantum phases [4–22], including those that are typically associated with strong repulsive interactions, e.g., antiferromagnetism (AF) [10–13] and d-wave SC [14–22].

In this Letter, we study a simple electron-phonon model, the "Holstein-Lieb" model (illustrated in Fig. 1), for which it is possible to obtain well-controlled results concerning the ground-state phase diagram (summarized in Fig. 2) through the use of an asymptotic strong-coupling expansion. Certain of the phases are interesting but not surprising—for instance, phonon-stabilized bipolarons can order (localize) to form a variety of valence bond solid (VBS) phases, or when the strongly coupled sites lie above the Fermi energy, they act as "negative U centers" that mediate SC pairing [23]. More unexpectedly, there is a range of parameters in which the problem maps onto a quantum dimer model [24,25] introduced by Rokshar and Kivelson (RK), and thus exhibits a variety of exotic "resonating valence-bond" (RVB) phases known to arise there, including (on the triangular lattice) a $\mathbb{Z}_2$ topologically ordered phase and (on the square lattice) a multicritical point which acts as the mother state for an infinite hierarchy of incommensurate phases. With this concrete example, we hope to suggest new avenues for the search for materials supporting "spin-liquid" phases [26] in systems with relatively strong electron-phonon couplings. To date, this effort has been almost entirely focused on studies of frustrated antiferromagnets.

We consider a Hamiltonian in which electrons can occupy orbitals on the vertices of the lattice, j, or on the bond centers between pairs of nearest-neighbor sites, $\langle ij\rangle$:

$$\hat{H} = -t\sum_{\langle ij\rangle\sigma}[\hat{f}^{\dagger}_{\langle ij\rangle\sigma}(\hat{c}_{i\sigma} + \hat{c}_{j\sigma}) + \text{H.c.}] + \sum_{\langle ij\rangle}(\mathcal{E} + \alpha\hat{X}_{\langle ij\rangle})\hat{n}_{\langle ij\rangle} + \hat{H}_{\text{ph}} \tag{1}$$

where $\hat{c}_{i\sigma}$ ($\hat{f}_{\langle ij\rangle\sigma}$) annihilates a spin-$\sigma$ electron on the orbital at site i (bond $\langle ij\rangle$), and $\hat{n}_i$ or $\hat{n}_{\langle ij\rangle}$ are the electron numbers on the corresponding orbitals. $\hat{X}_{\langle ij\rangle}$ are the coordinate operators of optical phonons on bonds described by the Hamiltonian:

$$\hat{H}_{\text{ph}} = \sum_{\langle ij\rangle}\left[\frac{K\hat{X}^2_{\langle ij\rangle}}{2} + \frac{\hat{P}^2_{\langle ij\rangle}}{2M}\right]. \tag{2}$$

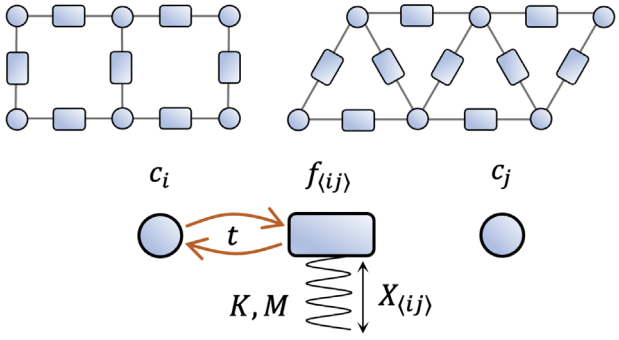

FIG. 1. An illustration of the Lieb lattices studied in this Letter, and the Holstein-Lieb model in Eq. (1).

By rescaling variables it is easy to see that there are precisely four independent energy scales in the problem: the band-structure scale t, the charge transfer gap $\mathcal{E}$, the phonon frequency, $\omega_0 \equiv \sqrt{K/M}$, and the phonon-induced electronic attraction, $U_{e\text{-ph}} \equiv \alpha^2/K$, which is the relevant measure of the electron-phonon coupling strength. We will perform a controllable strong-coupling analysis assuming $|t|$ to be a small energy scale (the precise meaning of this assumption will be made clear below), and obtain effective theories for the active degrees of freedom in different parameter regimes. At the end of the Letter, we will discuss the robustness of the results in the presence of additional couplings that are likely to be present in candidate materials.

Methods.—The effects of strong electron-phonon coupling can best be addressed following a unitary transformation [27]

$$\hat{U} \equiv \exp\left[i\frac{\alpha}{K}\sum_{\langle ij\rangle}\hat{P}_{\langle ij\rangle}\hat{n}_{\langle ij\rangle}\right], \tag{3}$$

that transforms the Hamiltonian into

$$\hat{U}^\dagger \hat{H}\,\hat{U} = -t\sum_{\langle ij\rangle\sigma}[\hat{D}_{\langle ij\rangle}\hat{f}^\dagger_{\langle ij\rangle\sigma}(\hat{c}_{i\sigma}+\hat{c}_{j\sigma}) + \text{H.c.}] + \sum_{\langle ij\rangle}\left[\mathcal{E}\hat{n}_{\langle ij\rangle} - \frac{U_{e\text{-ph}}}{2}\hat{n}^2_{\langle ij\rangle}\right] + \hat{H}_{\text{ph}}. \tag{4}$$

The resulting theory contains a unitary operator $\hat{D}_{\langle ij\rangle} \equiv e^{-i\hat{P}_{\langle ij\rangle}\alpha/K}$ that displaces the phonon coordinate by α/K. We will perform a perturbative analysis treating the second line in Eq. (4) as the unperturbed Hamiltonian, $\hat{H}_0$, and the first line as perturbations, $\hat{H}'$. Under most circumstances, $\hat{H}_0$ has an extensive ground-state degeneracy, so we use degenerate perturbation theory to derive an effective model acting in the degenerate subspace. We note that all the virtual processes, including those with phonon excitations, are included in this analysis. We keep terms in powers of t to the lowest order needed to resolve the degeneracy, and the validity of each model will be analyzed in each scenario. Since $\hat{H}$ can be defined on any lattice in any dimension, so can the resulting effective theories. Here, to be explicit, we will confine ourselves to the square and triangular lattices in two dimensions.

The first step in our analysis is to identify the degenerate ground-state manifold of $\hat{H}_0$, which we call $\mathcal{H}_0$; we will restrict our attention to the range of electron densities per unit cell, $0 < n \leq 2$. For convenience, we define $\mathcal{E}_1 \equiv \mathcal{E} - U_{e\text{-ph}}/2$ and $\mathcal{E}_2 \equiv 2\mathcal{E} - 2U_{e\text{-ph}}$ to represent the energies of a singly or doubly occupied bond orbital, and $\mathcal{E}_{12} \equiv \mathcal{E}_1 - \mathcal{E}_2 = 3U_{e\text{-ph}}/2 - \mathcal{E}$ to represent their energy difference. Because $\mathcal{E}_2 - 2\mathcal{E}_1 = -U_{e\text{-ph}}$ is always negative, singly occupied bond orbitals are always disfavored. Therefore, depending on the sign of $\mathcal{E}_2$, bond or site orbitals are favored, so that all possible occupation configurations of bond dimers or site electrons form a basis of $\mathcal{H}_0$.

For the case where bond dimers are active degrees of freedom ($\mathcal{E}_2 \lesssim 0$), there are two sorts of terms that will be generated by the perturbative analysis: There are diagonal terms (dimer potential energy) and off-diagonal terms (dimer kinetic energy). Since the phonon displacements are different for different dimer configurations, all off-diagonal terms must vanish in the limit of nondynamical phonons, $\omega_0 = 0$. Specifically, the amplitude of any process in which a dimer relocates onto or off of a bond is accompanied by a Frank-Condon factor F [28] defined as

$$F \equiv \langle 0|\hat{D}^2|0\rangle = e^{-X}, \tag{5}$$

where $|0\rangle$ is the ground state of the phonon Hamiltonian on the bond, and $X \equiv U_{e\text{-ph}}/\omega_0$ is a dimensionless factor quantifying the degree of retardation, and the displacement operator $\hat{D}$ is squared since the occupancy of the orbital changes by two electrons. This factor becomes arbitrarily small in the limit of strong retardation. On the other hand, the potential terms always only receive $\mathcal{O}(1)$ factors from the virtual phonon fluctuations.

Below we derive the effective theories and obtain expressions as functions of the bare energy scales for the coupling constants that arise in low-order perturbation theory in t. The effective Hamiltonians are given in Eqs. (6), (8), and (9). The asymptotic expressions and the limiting behaviors in the small and large ω_0 limits of the effective couplings are given in Table I. Their explicit expressions and derivations are deferred to the Supplemental Material [29].

$U_{e\text{-ph}} > \mathcal{E}$: *dimer models.*—In this case, the energy necessary for breaking a dimer is $\mathcal{E}_{12}$; thus the expansion series in t is controllable as long as $t \ll \mathcal{E}_{12}$. For a dimer on bond $\langle ij\rangle$, we define the annihilation operator as $\hat{b}_{\langle ij\rangle} \equiv \hat{f}_{\langle ij\rangle\uparrow}\hat{f}_{\langle ij\rangle\downarrow}$ and the dimer occupation number operator $\hat{n}^b_{\langle ij\rangle} \equiv \hat{b}^\dagger_{\langle ij\rangle}\hat{b}_{\langle ij\rangle} = 0, 1$. To the fourth order in t, we obtain the following model for the dimers:

$$\hat{H}_b = \sum_{\langle ijk\rangle}[-\tau_1(\hat{b}^\dagger_{\langle ij\rangle}\hat{b}_{\langle jk\rangle} + \text{H.c.}) + V_1\hat{n}^b_{\langle ij\rangle}\hat{n}^b_{\langle jk\rangle}] \tag{6}$$

where the summation is over all pairs of nearest-neighbor bonds with a single vertex in common, and it is implicit that we have omitted terms of order t^6 and higher, to which we shall return shortly. Therefore, we obtain a hard-core boson model on the bond lattice with repulsive interactions.

As shown in Table I, when $X \lesssim 1$ it follows that $\tau_1 \sim V_1$, so this is an interacting problem with no small parameter to give theoretical control. We label this region "Interacting dimers" in Fig. 2. For $n \ll 1$, the ground state is presumably an s-wave superfluid, independent of the details of the

TABLE I. Asymptotic expressions and limiting behaviors of the coefficients in the effective theories in Eqs. (6), (8), and (9). Each limiting behavior is evaluated in the region of validity of the corresponding effective Hamiltonian.

	Antiadiabatic	Adiabatic
	$\omega_0 \to \infty$, $X \to 0$	$\omega_0 \to 0$, $X \to \infty$
$t_{\text{eff}} \sim (t^2/\mathcal{E}_1)$	$t^2/\mathcal{E}_1$	$t^2/\mathcal{E}$
$\tau_0 \sim (2t^2F/\mathcal{E}_1)$	$2t^2/\mathcal{E}_1$	$(\sqrt{\pi X}t^2/\mathcal{E}_1)e^{-X} \to 0$
$\tau_1 \sim (t^4F^2/\mathcal{E}_{12}^3)$	$\{[4t^4(2U_{e\text{-ph}} - \mathcal{E})]/[\mathcal{E}_{12}^2\lvert\mathcal{E}_2\rvert U_{e\text{-ph}}]\}$	$\{[4\sqrt{2\pi X}t^4]/[\mathcal{E}_2^2U_{e\text{-ph}}]\}e^{-2X} \to 0$
$V_1 \sim [t^4/\mathcal{E}_{12}^3]$	$[4t^4(5U_{e\text{-ph}}/2 - \mathcal{E})]/[\mathcal{E}_{12}^3U_{e\text{-ph}}]$	$[2t^4(4U_{e\text{-ph}} - \mathcal{E})]/[(2U_{e\text{-ph}} - \mathcal{E})^3U_{e\text{-ph}}]$
$J_{\text{eff}} \sim (t^4/\mathcal{E}_1^3)$	$4t^4U_{e\text{-ph}}/\mathcal{E}_1^3\mathcal{E}_2$	$t^4U_{e\text{-ph}}^3/2\mathcal{E}_1^2\mathcal{E}^4$

lattice structure and the interactions. As n approaches 1, the balance between the interactions and the kinetic terms becomes more subtle. Similar models have been studied on several lattices [33–38], where various superfluid, charge, and supersolid orders were found. We expect analogous phases to arise in the present model.

However, when X is large, such that $F \ll 1$, the V_1 term is dominant over τ_1. Those ground states of V_1 within $\mathcal{H}_0$ form an emergent low-energy (still extensively degenerate) subspace, $\mathcal{H}_1$, in which, as in the RK quantum dimer models, no more than one dimer can touch a given site. Within $\mathcal{H}_1$, we further perform perturbative analysis on square and triangular lattices and obtain the RK model as the effective model:

$$\hat{H}_{\text{RK}} = V_2 \sum_{\square} [|\square\rangle\langle\square| + |\square\rangle\langle\square|] - \tau_2 \sum_{\square} [|\square\rangle\langle\square| + |\square\rangle\langle\square|] \tag{7}$$

where the ket (bra) represents a pair of annihilation (creation) operators on the thickened bonds, and the summation is over all possible four-sided plaquettes. To leading order in τ_1/V_1, it is easy to see that $\tau_2 = (4\tau_1^2/V_1) \sim (t^4/\mathcal{E}_{12}^3)F^4$. In terms of the same expansion, one would conclude that $V_2 = \mathcal{O}(\tau_1^5/V_1^4)$ is always small compared to τ_2. However, since we are simultaneously assuming both t and F are small, we need to consider terms [not shown in Eq. (6)] that are higher order in t, but which are not suppressed by F (potential terms). (See Fig. 3 for illustrations of the virtual processes that contribute to the effective theory.) Since it involves such high-order processes, it is not worth writing out explicitly the results. What is essential is that the leading term only contributes to V_2 and it is eighth order in t and positive, i.e., $V_2 \sim (t^8/\mathcal{E}_{12}^7)$ [39]. From the perturbative perspective, there are two types of leading virtual process, both of which contribute positively to V_2: If two dimers occupy two parallel sides of a four-sided plaquette, the lowest order virtual process that nontrivially connects them is a ring exchange of

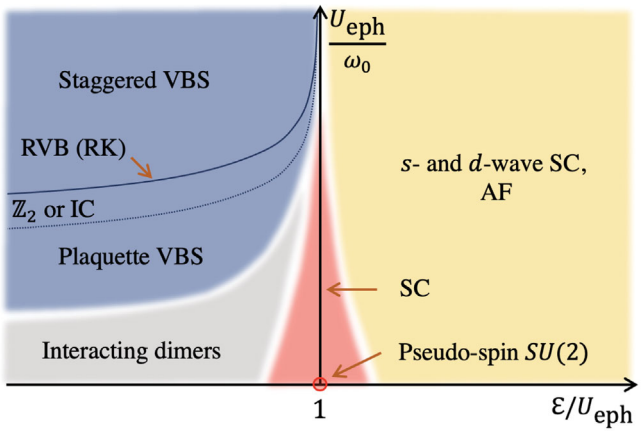

FIG. 2. Schematic $T = 0$ phase diagram for $n = 1$ in the small $|t|$ limit as a function of the dimensionless ratios of parameters in the model, Eq. (1); the vertical axis quantifies the degree of retardation and the horizontal axis the strength of the electron-phonon coupling. The blue region on the left top is described by the quantum dimer model in Eq. (7). The yellow region on the right is described by the weakly interacting theory in Eq. (8). The red region in the middle is described by Eq. (9) and is confined to a narrow window. The grey region on the left bottom is described by the effective bosonic Hamiltonian, Eq. (6), where controlled analysis of the ground-state phases is missing. The RK line, which corresponds to the exactly solvable point $V_2 = \tau_2$ in Eq. (7), occurs with moderately large retardation, $U_{e\text{-ph}}/\omega_0 = \mathcal{O}[\ln(\mathcal{E}_{12}/t)]$, as long as $\mathcal{E}/U_{e\text{-ph}}$ is not close to 1. The $\mathbb{Z}_2$ symbol represents a $\mathbb{Z}_2$ spin-liquid phase on the triangular lattice, and IC stands for possible incommensurate crystalline phases on the square lattice.

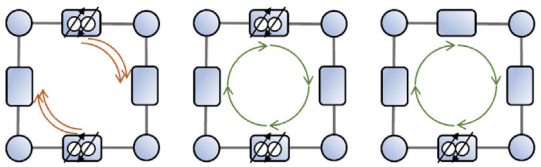

FIG. 3. Illustration of the virtual processes (arrows indicate the direction of electron hops) on a four-sided plaquette contributing to the terms in the RK effective theory in Eq. (7). The first class contributes to τ_2 while the latter two contribute to V_2.

electrons, which results in a fermion minus sign that turns what would have been an energy gain into a cost. On the other hand, if only one dimer occupies a side of a plaquette, there is an allowed virtual process in which a single electron travels around the plaquette—this energy-gaining process is blocked when there are two dimers on the plaquette. Both processes are eighth order in t on the lattices we are considering. (We have performed exact diagonalization studies on small clusters in the limit $\omega_0 = 0$ as a check of these conclusions).

Formally, we can consider $\hat{H}_{\mathrm{RK}}$ to be the effective Hamiltonian in an asymptotic limit where $F \sim |t|/\mathcal{E}_{12} \sim \delta \ll 1$, such that the couplings τ_2 and V_2 are both of order δ^8, with relative magnitudes that can be tuned in a wide range—for instance by varying ω_0. All omitted terms are higher order in powers of δ.

The zero-temperature phase diagrams of the quantum dimer models Eq. (7) on the square and triangular lattices have been solved, with results we briefly summarize here. For both cases, the line along which $\tau_2 = V_2$ is special (corresponding to the RK point [24,25]) and is labeled "RK" in Fig. 2. Here, an exact ground state is an equal amplitude superposition of all dimer configurations in a given topological sector, i.e., a short-ranged RVB state [26]. The ground states in different topological sectors are exactly degenerate, which leads to topological degeneracy on compact manifolds. Through exact evaluations of the dimer correlations [40–42], it is known that this point is gapless on the square lattice and gapped on the triangular lattice.

Further numerical and analytical investigations have fleshed out the full phase diagram of this model. On the square lattice, for the model defined in Eq. (7), the RK point is a critical point separating two different VBS states: staggered (for $V_2 > \tau_2 > 0$) and plaquette (for $0 < V_2 < \tau_2$) [43,44]. More generally, it is an unstable multicritical point described by the quantum Lifshitz model [42,45], near which a wide class of perturbations can induce incommensurate crystalline phases through a mechanism known as Cantor deconfinement [45,46]. We label the region that may host such additional phases "IC" in Fig. 2 [47]. On the triangular lattice, the RK point lies on the boundary of a phase that exhibits $\mathbb{Z}_2$ topological order in a range of $\nu_c\tau_2 < V_2 < \tau_2$ with $\nu_c \lesssim 0.8$ (marked $\mathbb{Z}_2$ in Fig. 2); two different VBSs occur for other ranges of parameters: staggered (for $V_2 > \tau_2 > 0$) and $\sqrt{12} \times \sqrt{12}$ (for $0 < V_2 < \nu_c\tau_2$) [49,50], which we also refer to as "plaquette VBS" in the schematic phase diagram Fig. 2.

The $\mathbb{Z}_2$ spin liquid is known to have several types of excitations: spinons, holons, and visions. In the current case, while visions have relatively low creation energy $\sim\tau_2$, the creation of spinons or holons carries a large energy cost $\sim\mathcal{E}_2$ or $\sim U_{e\text{-ph}}$ in order to break a dimer. Therefore, when lightly doping holes into the system near the RK point such that $|n-1| = x \ll 1$, we will likely have dimer vacancies as charge carriers leading to condensation with SC T_c determined by the coherence scale, $T_c \sim x\tau_1 \sim x(t^6/\mathcal{E}_{12}^5)$ [51]. For the square lattice RK model, exactly at the RK point, there are also gapless "resonon" excitations with momenta near (π, π) and a quadratic dispersion. Since the motion of the dimers is tied to that of the phonons, the emergence of such excitations should be observable in measurements of the phonon spectrum, e.g., through neutron scattering.

$U_{e\text{-ph}} < \mathcal{E}$: *weakly interacting model.*—In this case, the effective model is expressed in terms of site electrons. To fourth order in t, the effective Hamiltonian is

$$\hat{H}_c = -t_{\mathrm{eff}} \sum_{\langle ij\rangle\sigma} (\hat{c}^\dagger_{i\sigma}\hat{c}_{j\sigma} + \mathrm{H.c.}) - 2J_{\mathrm{eff}} \sum_{\langle ij\rangle} \hat{n}_{[i+j]\uparrow}\hat{n}_{[i+j]\downarrow} \quad (8)$$

where $\hat{n}_{[i+j]\sigma} \equiv (\hat{c}^\dagger_{i\sigma} + \hat{c}^\dagger_{j\sigma})(\hat{c}_{i\sigma} + \hat{c}_{j\sigma})/2$ is the number of electrons in a bonding orbital between sites i and j. Since any virtual movement of electrons necessarily costs $\mathcal{E}_1$ in the intermediate state, the expansion is valid as long as $|t| \ll \mathcal{E}_1$. As can be seen from Table I, t_{eff} is second order in t and J_{eff} is fourth order. Thus, we should consider this theory in its weak coupling limit, $J_{\mathrm{eff}} \ll t_{\mathrm{eff}}$.

With detailed discussion in the Supplemental Material [29], we analyze the weak-coupling instabilities in the context of a Hartree-Fock mean-field analysis that is reasonable in this limit. We find that, on square and triangular lattices, s-wave SC is always the dominant instability for $n < 2$. However, when $n \approx 1$ on the square lattice, there is also a d-wave pairing state that is only moderately subdominant to the dominant s-wave channel. This competition between the s- and d-wave paired states can be tuned by the additional weak Hubbard repulsion on site orbitals, U_c; when $U_c \gtrsim 2.2J_{\mathrm{eff}}$, the d-wave paired state has the lower variational energy. Exactly at $n = 1$, there is also an AF instability, which is also subdominant to the s-wave SC instability, but which is favored over all superconducting states when $U_c > 2J_{\mathrm{eff}}$.

$U_{e\text{-ph}} \approx \mathcal{E}$: *monomer-dimer model.*—In the narrow region $|\mathcal{E}_2| \lesssim \tau_0$, where τ_0 (again given in Table I) is the matrix element for converting a pair of site electrons to a pair of bond electrons, both c and f orbitals are active. The effective Hamiltonian in this case is

$$\begin{aligned}\hat{H}_{bc} = &\sum_{\langle ij\rangle} [t_{\mathrm{eff}}(2\hat{n}^b_{\langle ij\rangle} - 1)2\hat{n}_{[i+j]} + (\mathcal{E}_2 - 4t_{\mathrm{eff}})\hat{n}^b_{\langle ij\rangle}] \\ &+ \tau_0 \sum_{\langle ij\rangle} [\hat{b}^\dagger_{\langle ij\rangle}(\hat{c}_{i\uparrow} + \hat{c}_{j\uparrow})(\hat{c}_{i\downarrow} + \hat{c}_{j\downarrow}) + \mathrm{H.c.}]. \end{aligned} \quad (9)$$

In this regime, no controllable analysis can be performed. A mean-field analysis, treating b and c as decoupled, suggests an s-wave SC phase—presumably one that connects to the corresponding phase in the $U_{e\text{-ph}} < \mathcal{E}$ case.

It is interesting to note that, for arbitrary t, there is a hidden pseudospin $SU(2)$ symmetry in the original

problem when $\mathcal{E}_2 = 0$ and $X \to 0$ (marked with the red circle in Fig. 2), which is a generalization of that of the Hubbard model on bipartite lattices [30,31]. This symmetry implies, in the thermodynamic limit, for the ground state of the system at *any filling*

$$\frac{1}{N_{\text{site}}^2}\left\langle \left| \sum_i \hat{c}_{i\uparrow}\hat{c}_{i\downarrow} - \sum_{\langle ij\rangle} \hat{f}_{\langle ij\rangle\uparrow}\hat{f}_{\langle ij\rangle\downarrow} \right|^2 \right\rangle = 0 \qquad (10)$$

which is, as discussed in detail in the Supplemental Material [29], difficult to satisfy in any SC state that does not have space-dependent oscillations in sign.

Outlook.—The derivations of the effective theories can be easily generalized to include *strong* (in comparison to t) or even infinite Hubbard repulsion, U_e, on the site orbitals. In that case, the model corresponding to $U_{e\text{-ph}} < \mathcal{E}$ at $n \lesssim 1$ is a $t-J$ model (with no double occupancy constraint on site orbitals). The AF coupling J in this model is *enhanced* by the effective attraction on the bond orbitals, and an extra nearest-neighbor density-density repulsion interaction is induced by phonon virtual fluctuations. On the other hand, the dimer models for $U_{e\text{-ph}} > \mathcal{E}$ are not qualitatively changed by the presence of a repulsive Hubbard interaction on site and bond orbitals, nor weak further-ranged hopping and electron-phonon coupling, as long as $\mathcal{H}_0$ is unaffected.

In considering the search for spin-liquid phases in real materials featuring significant electron-phonon couplings, we summarize the key ingredients that we think are crucial for the mechanism revealed in this Letter: (1) atomic-scale structures with electronically active atoms on both vertices and the bridging sites between them (it is encouraging to note that a large class of real materials have this feature [55–57]); (2) strong coupling to phonon modes on bonds that allow the formation of bipolarons localized on bonds; (3) a moderately large degree of retardation that suppresses the quantum hopping relative to interactions and thus leads to constraints on the low-energy Hilbert space. Furthermore, we would like to point out that these ideas [especially (1) and (3)] can be adopted in the design of quantum simulation experiments as a novel way of realizing geometrical blockade analogous to the concept in Rydberg systems, which was crucial to a realization of spin-liquid state in a recent experiment [58,59]. In that context, the phonon degrees of freedom could be replaced by various other bosonic modes.

We thank Oskar Vafek, Ruben Verresen, Hong Yao, Kyung-Su Kim, and John Sous for helpful discussions. S. A. K. was supported, in part, by NSF Grant No. DMR-2000987 at Stanford.

[1] J. Bardeen, L. N. Cooper, and J. R. Schrieffer, Phys. Rev. **108**, 1175 (1957).
[2] W. P. Su, J. R. Schrieffer, and A. J. Heeger, Phys. Rev. Lett. **42**, 1698 (1979).
[3] A. J. Heeger, S. Kivelson, J. R. Schrieffer, and W. P. Su, Rev. Mod. Phys. **60**, 781 (1988).
[4] J. Sous, M. Chakraborty, R. V. Krems, and M. Berciu, Phys. Rev. Lett. **121**, 247001 (2018).
[5] Z. Han, S. A. Kivelson, and H. Yao, Phys. Rev. Lett. **125**, 167001 (2020).
[6] K. S. Huang, Z. Han, S. A. Kivelson, and H. Yao, npj Quantum Mater. **7**, 1 (2022).
[7] Z. Han and S. A. Kivelson, Phys. Rev. B **105**, L100509 (2022).
[8] Z.-X. Li, M. L. Cohen, and D.-H. Lee, Phys. Rev. B **100**, 245105 (2019).
[9] A. Blason and M. Fabrizio, Phys. Rev. B **106**, 235112 (2022).
[10] X. Cai, Z.-X. Li, and H. Yao, Phys. Rev. Lett. **127**, 247203 (2021).
[11] A. Götz, S. Beyl, M. Hohenadler, and F. F. Assaad, Phys. Rev. B **105**, 085151 (2022).
[12] X. Cai, Z.-X. Li, and H. Yao, Phys. Rev. B **106**, L081115 (2022).
[13] Q.-G. Yang, D. Wang, and Q.-H. Wang, Phys. Rev. B **106**, 245136 (2022).
[14] J. Song and J. F. Annett, Phys. Rev. B **51**, 3840 (1995).
[15] T. P. Devereaux, A. Virosztek, and A. Zawadowski, Phys. Rev. B **51**, 505 (1995).
[16] H. Kamimura, S. Matsuno, Y. Suwa, and H. Ushio, Phys. Rev. Lett. **77**, 723 (1996).
[17] N. Bulut and D. J. Scalapino, Phys. Rev. B **54**, 14971 (1996).
[18] M. Mierzejewski, J. Zieliński, and P. Entel, Phys. Rev. B **53**, 431 (1996).
[19] C. Honerkamp, H. C. Fu, and D.-H. Lee, Phys. Rev. B **75**, 014503 (2007).
[20] Z. B. Huang, H. Q. Lin, and E. Arrigoni, Phys. Rev. B **83**, 064521 (2011).
[21] F. Wu, A. H. MacDonald, and I. Martin, Phys. Rev. Lett. **121**, 257001 (2018).
[22] R. T. Clay and D. Roy, Phys. Rev. Res. **2**, 023006 (2020).
[23] T. Geballe and S. Kivelson, in *Pwa90: A Lifetime of Emergence* (World Scientific, Singapore, 2016), pp. 127–133.
[24] D. S. Rokhsar and S. A. Kivelson, Phys. Rev. Lett. **61**, 2376 (1988).
[25] R. Moessner and K. S. Raman, in *Introduction to Frustrated Magnetism* (Springer, New York, 2011), pp. 437–479.
[26] L. Savary and L. Balents, Rep. Prog. Phys. **80**, 016502 (2016).
[27] I. Lang and Y. A. Firsov, Sov. Phys. JETP **16**, 1301 (1963), http://www.jetp.ras.ru/cgi-bin/e/index/e/16/5/p1301?a=list.
[28] E. Carlson, V. Emery, S. Kivelson, and D. Orgad, in *Superconductivity* (Springer, New York, 2008), pp. 1225–1348.
[29] See Supplemental Material at http://link.aps.org/supplemental/10.1103/PhysRevLett.130.186404 and Refs. [5,30–32] therein for explicit derivations and expressions for the effective coefficients, the detailed discussion on the pseudo-spin symmetry, and the mean-field analysis of the weakly interacting model.
[30] C. N. Yang, Phys. Rev. Lett. **63**, 2144 (1989).
[31] S. Zhang, Phys. Rev. Lett. **65**, 120 (1990).

[32] D. F. Agterberg, J. S. Davis, S. D. Edkins, E. Fradkin, D. J. Van Harlingen, S. A. Kivelson, P. A. Lee, L. Radzihovsky, J. M. Tranquada, and Y. Wang, Annu. Rev. Condens. Matter Phys. **11**, 231 (2020).
[33] G. G. Batrouni and R. T. Scalettar, Phys. Rev. Lett. **84**, 1599 (2000).
[34] G. Schmid, S. Todo, M. Troyer, and A. Dorneich, Phys. Rev. Lett. **88**, 167208 (2002).
[35] Y.-C. Chen, R. G. Melko, S. Wessel, and Y.-J. Kao, Phys. Rev. B **77**, 014524 (2008).
[36] R. G. Melko, A. Paramekanti, A. A. Burkov, A. Vishwanath, D. N. Sheng, and L. Balents, Phys. Rev. Lett. **95**, 127207 (2005).
[37] F. Wang, F. Pollmann, and A. Vishwanath, Phys. Rev. Lett. **102**, 017203 (2009).
[38] S. Wessel, Phys. Rev. B **75**, 174301 (2007).
[39] As an aside, we note that a π external magnetic flux per plaquette will turn this repulsion into attraction.
[40] P. Fendley, R. Moessner, and S. L. Sondhi, Phys. Rev. B **66**, 214513 (2002).
[41] M. E. Fisher and J. Stephenson, Phys. Rev. **132**, 1411 (1963).
[42] E. Fradkin, *Field Theories of Condensed Matter Physics* (Cambridge University Press, Cambridge, England, 2013).
[43] A. Ralko, D. Poilblanc, and R. Moessner, Phys. Rev. Lett. **100**, 037201 (2008).
[44] Z. Yan, Z. Zhou, O. F. Syljuåsen, J. Zhang, T. Yuan, J. Lou, and Y. Chen, Phys. Rev. B **103**, 094421 (2021).
[45] E. Fradkin, D. A. Huse, R. Moessner, V. Oganesyan, and S. L. Sondhi, Phys. Rev. B **69**, 224415 (2004).
[46] S. Papanikolaou, K. S. Raman, and E. Fradkin, Phys. Rev. B **75**, 094406 (2007).
[47] We note that these relevant terms generically exist in the higher-order terms that are neglected in this study. It is also worth noting that the inclusion of a small admixture of further (second neighbor) range dimers can stabilize a $\mathbb{Z}_2$ spin-liquid phase proximate to the RK point, similar to that seen in the triangular lattice [48].
[48] H. Yao and S. A. Kivelson, Phys. Rev. Lett. **99**, 247203 (2007).
[49] R. Moessner and S. L. Sondhi, Phys. Rev. Lett. **86**, 1881 (2001).
[50] A. Ralko, M. Ferrero, F. Becca, D. Ivanov, and F. Mila, Phys. Rev. B **71**, 224109 (2005).
[51] We note that there can be rich physics for dilute doped holes [52–54] even from an ordered state, which should be analyzed more carefully in future studies.
[52] K.-S. Kim, Phys. Rev. B **107**, L140401 (2023).
[53] J. Sous and M. Pretko, Phys. Rev. B **102**, 214437 (2020).
[54] Z.-X. Li, S. G. Louie, and D.-H. Lee, Phys. Rev. B **107**, L041103 (2023).
[55] R. Fan, L. Sun, X. Shao, Y. Li, and M. Zhao, Chem. Phys. Mater. **2**, 30 (2022).
[56] T. Yang, Y. Z. Luo, Z. Wang, T. Zhu, H. Pan, S. Wang, S. P. Lau, Y. P. Feng, and M. Yang, Nanoscale **13**, 14008 (2021).
[57] X. Li, Q. Li, T. Ji, R. Yan, W. Fan, B. Miao, L. Sun, G. Chen, W. Zhang, and H. Ding, Chin. Phys. Lett. **39**, 057301 (2022).
[58] R. Verresen, M. D. Lukin, and A. Vishwanath, Phys. Rev. X **11**, 031005 (2021).
[59] G. Semeghini, H. Levine, A. Keesling, S. Ebadi, T. T. Wang, D. Bluvstein, R. Verresen, H. Pichler, M. Kalinowski, R. Samajdar, A. Omran, S. Sachdev, A. Vishwanath, M. Greiner, V. Vuletić, and M. D. Lukin, Science **374**, 1242 (2021).